The Astronomical Journal, 145:14 (9pp), 2013 January doi:10.1088/0004-6256/145/1/14

BVR_cI_c OBSERVATIONS AND ANALYSES OF THE DWARF DETACHED BINARY V1043 CASSIOPEIA AND A COMMENT ON PRECONTACT W UMa'S

R. G. Samec[1], P. M. Smith[1], H. Chamberlain[1], D. R. Faulkner[2], and W. Van Hamme[3]
[1] Astronomy Group, Physics and Engineering Department, Bob Jones University, 1700 Wade Hampton Boulevard, Greenville, SC 29614, USA
[2] Division of Math, Science, Nursing & Public Health, University of South Carolina, Lancaster, 476 Hubbard Drive, Lancaster, SC 29720, USA
[3] Physics Department, Florida International University, 11200 SW 8th Street, Miami, FL 33199, USA
Received 2012 July 25; accepted 2012 October 29; published 2012 December 11

ABSTRACT

Complete Bessel BVR_cI_c light curves of V1043 Cassiopeia [2MASS J00371195 + 5301324, Mis V1292, USNO−A2.0 1425−00875743, $\alpha(2000) = 00^{\rm h}37^{\rm m}11\overset{\rm s}{.}95$, $\delta(2000) = +53^\circ01'32\overset{''}{.}5$] are analyzed. The system is a member of the small group of pre-contact W UMa binaries (PCWBs). Its light curve has the appearance of an Algol (EA) light curve, however it is made up of dwarf solar type components in a detached mode with a period of only 0.6616 days. The analysis includes a period study, an improved ephemeris, a mass ratio search, and a simultaneous BVR_cI_c Wilson–Devinney solution. We document about 20 other PCWBs given in the literature. Several have RS CVn-like properties.

Key words: binaries: close – binaries: eclipsing – stars: evolution – stars: individual (V1043 CAS)

Online-only material: color figure

1. INTRODUCTION

For the past 50 years, many journal articles have been published on solar-type contact binaries with their EW-type light curves. In addition, a number of papers have analyzed observations of solar-type *near* contact binaries. These solar-types are usually semidetached with the other component nearly filling, but still under-filling, its critical Roche lobe. These usually have EB-type light curves. All of these objects, taken as a whole, are referred to as W UMa binaries. They are thought to be the most abundant type of variable stars in the cosmos, comprising some 1% of all variable stars. The accepted scenario for these W UMa binaries is that they are undergoing steady but slow angular momentum losses due to magnetic braking as stellar winds travel radially away on stiff bipolar field lines. These binaries are believed to eventually coalesce into "reborn," single, fast rotating A-type stars (Guinan & Bradstreet 1988). This process of period decrease has been documented in many period studies, but certainly not all, as seen in $O - C$ diagrams. If we accept this scenario as typical of W UMa aging, then we would expect to find well-detached solar-type binaries early on in the braking process with *EA* light curves. We might refer to these objects as Pre-contact W UMa binaries (PCWBs). We recently analyzed such a system, V1001 Cas (Samec et al. 2012a). Indeed, this particular binary has a classical type Algol light curve (EA), with a period of only 0.43 days. It is well detached, with fill-outs of ∼70% and ∼85%, by potentials, and has a component temperature difference of ∼800 K. The spectral types of the stars are K4V and M3 (2)V. In this paper, we document another PCWB, V1043 Cas. A table summarizing other PCWBs is given.

2. HISTORY

Yoshida et al. (http://www.aerith.net/misao/data/misv.cgi?1292) discovered V1043 Cassiopeia [denoted as V in Figure 3, 2MASS J00371195 + 5301324, Mis V1292, USNO−A2.0 1425−00875743, $\alpha(2000) = 00^{\rm h}37^{\rm m}11\overset{\rm s}{.}93$, $\delta(2000) = +53^\circ01'32\overset{''}{.}8$]. It was reported by the MISAO Project (Nakajima et al. 2006) as having a 13.29–14.28 V mag range, and identified as an EB type with the following ephemeris:

$$\text{HJD } T_{\min} I = 2453300.9578 + 0.6616d \times E. \quad (1)$$

Their light curve is given in Figure 1. The USNO-A2.0 Catalogue gives an R magnitude of 13.0 and a B magnitude of 14.2. The system is named in the 80th GCVS Name List in Kazarovets et al. (2011). Further comment on the orbital evolution of the system's period cannot be addressed due to the paucity of timings and the brevity of the observational period. However, this system should be placed on observers' programs for timings of minimum light so that a history can be established which will determine whether or not this system has a decreasing period as one would expect if the binary is actually heading toward coalescence as believed for PCWBs.

3. OBSERVATIONS

Our BVR_cI_c observations were taken on 2010 September 28 and 29 at Lowell Observatory with the 0.81 m reflector on Anderson Mesa, outside Flagstaff with National Undergraduate Research Observatory (NURO) time and a CRYOTIGER cooled (<−100 C) 2KX2K CCD NASACAM. Individual observations included 206 in B, 209 in V, 208 in R_c, and 206 in I_c. The standard error of a single observation was 4 mmag in V, 3 mmag in R_c and I_c, and 7 mmag in B. Nightly images were calibrated with 25 bias frames, five flat frames in each filter, and ten 300 s dark frames. Exposure times were 150 s in B, 45 s in V, 40 s in R_c, and 40 s in I_c. Figure 2 shows sample observations of B, V, and $B - V$ color curves on the night of 2010 September 29. Our observations are given in Table 1, in delta magnitudes, ΔB, ΔV, ΔR_c, and ΔI_s, in the sense of variable minus comparison star.

4. FINDING CHART

The comparison star, C [(GSC 3654 0269) [$\alpha(2000) = 00^{\rm h}37^{\rm m}2\overset{\rm s}{.}5367$, $\delta(2000) = +52^\circ59'44\overset{''}{.}686$], $V = 11.350$ (0.087). $B - V = 0.397$ (TYCHO)] and check star, K (GSC 3654 0185) [$\alpha(2000) = 00^{\rm h}36^{\rm m}21\overset{\rm s}{.}6094$, $\delta(2000) = +52^\circ59'50\overset{''}{.}815$], $V = 10.837(0.065)$, $B - V = 0.886$ (0.088) (TYCHO)] were

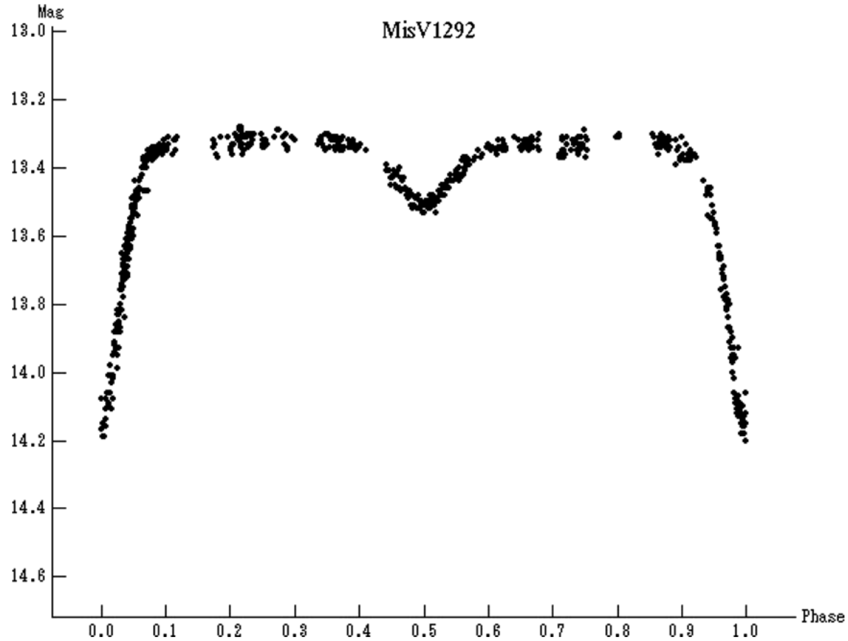

Figure 1. Mis V1292 light curve.

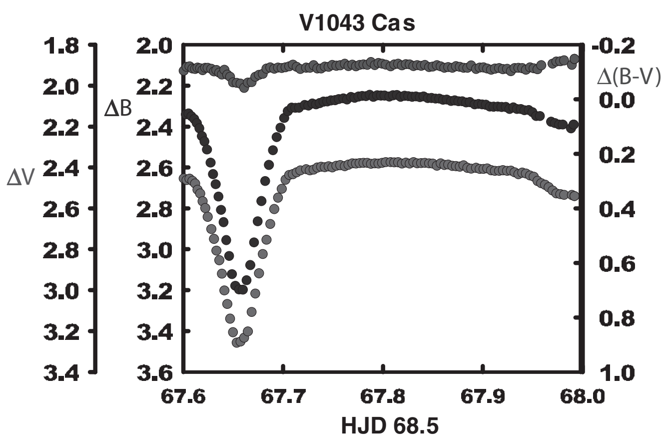

Figure 2. *B*, *V*, and $B - V$ color curves of V1043 Cas on the night of 2010 September 29.

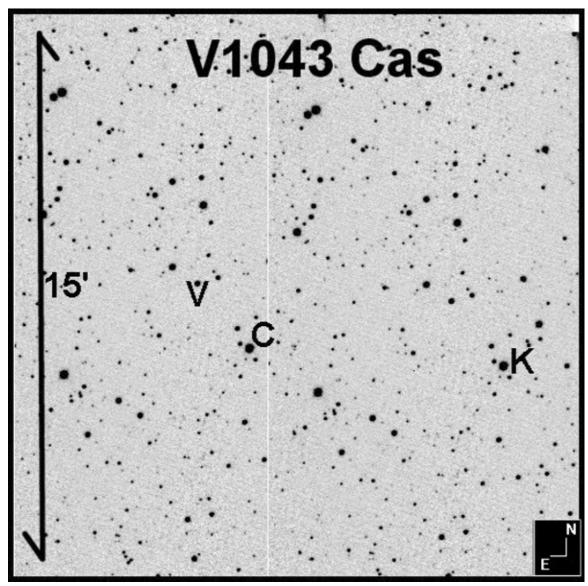

Figure 3. Finding Chart of V1043 Cas including variable (*V*), comparison (*C*), and check Stars (*K*).

chosen in the same field (($V - C$) has $|\Delta(B - V)| < 0.2$) as designated on the finding chart included for the convenience of future observers as in Figure 3.

5. PERIOD DETERMINATION

Four times of minimum light were computed from our observations, two primary and two secondary eclipses. These were calculated from parabola fits and then averages of *B*, *V*, R_c, and I_c determinations. These are given in Table 2 with standard errors given in parentheses. The other eclipse timings are listed in the table. The following precision linear ephemeris, Equation (2), was calculated from all of the available eclipse timings:

$$\text{HJD } T_{\min} \text{ I} = 24555467.6567 \pm 0.0010 + 0.66158617 \pm 0.00000047 d^{*} E \quad (2)$$

$$\text{HJD } T_{\min} \text{ I} = 24555467.65748 \pm 0.00001 + 0.6615992 \pm 0.000054 d^{*} E. \quad (3)$$

Equation (3) was a fitting equation to the light curve calculated from the Wilson program. An $O - C$ plot of the linear residuals from Equation (2) is shown in Figure 4. The complete listing of the calculation for the $O - C$ plot is given in Table 2. Equation (2) above represents a high-precision, improved linear ephemeris of the variable.

6. LIGHT CURVES AND TEMPERATURE DETERMINATION

The light curves were phased using Equation (2). These are shown in Figures 5(a) and (b). Light curve amplitudes and the differences in maxima and minima are given in Table 3. The primary amplitudes vary from $V = 0.95$ to 0.74 mag for *I* while the secondary amplitudes are only 0.16 (*B*) to 0.25 (*I*). The O'Connell effect varies from 4% to 5%, revealing that there

Table 1
Photometry of V1043 CAS

BDM	BHJD 2455400 +	BDM	BHJD 2455400 +	BDM	BHJD 2455400 +	BDM	BHJD 2455400 +	BDM	BHJD 2455400 +
2.350	67.5995	2.279	67.7404	2.292	67.8994	2.344	68.6776	2.307	68.8552
2.341	67.6024	2.278	67.7442	2.294	67.9031	2.338	68.6815	2.309	68.8594
2.337	67.6053	2.273	67.7479	2.303	67.9071	2.325	68.6858	2.313	68.8633
2.350	67.6081	2.272	67.7520	2.304	67.9108	2.317	68.6897	2.312	68.8675
2.364	67.6110	2.266	67.7557	2.303	67.9150	2.310	68.6938	2.318	68.8714
2.384	67.6135	2.263	67.7603	2.305	67.9188	2.311	68.6977	2.314	68.8754
2.409	67.6161	2.268	67.7640	2.305	67.9231	2.304	68.7018	2.322	68.8793
2.447	67.6186	2.256	67.7679	2.314	67.9268	2.306	68.7057	2.324	68.8863
2.473	67.6211	2.260	67.7717	2.307	67.9306	2.309	68.7115	2.324	68.8902
2.513	67.6237	2.254	67.7755	2.315	67.9343	2.300	68.7154	2.329	68.8946
2.577	67.6273	2.251	67.7792	2.315	67.9381	2.298	68.7204	2.325	68.8985
2.633	67.6298	2.252	67.7830	2.321	67.9418	2.304	68.7243	2.333	68.9026
2.682	67.6324	2.245	67.7867	2.320	67.9460	2.306	68.7297	2.330	68.9065
2.743	67.6352	2.256	67.7904	2.330	67.9497	2.301	68.7336	2.340	68.9113
2.808	67.6378	2.248	67.7942	2.349	67.9535	2.302	68.7376	2.339	68.9152
2.868	67.6403	2.249	67.7979	2.171	67.9648	2.302	68.7415	2.349	68.9195
2.956	67.6430	2.249	67.8016	2.377	67.9685	2.305	68.7455	2.343	68.9234
3.033	67.6459	2.254	67.8064	2.384	67.9723	2.301	68.7494	2.344	68.9274
3.122	67.6487	2.248	67.8101	2.391	67.9764	2.306	68.7534	2.347	68.9313
3.179	67.6521	2.246	67.8139	2.391	67.9801	2.312	68.7573	2.385	68.9367
3.197	67.6558	2.255	67.8176	2.409	67.9884	2.305	68.7620	2.428	68.9406
3.198	67.6596	2.250	67.8217	2.391	67.9910	2.304	68.7659	2.567	68.9496
3.152	67.6633	2.252	67.8254	2.297	68.5949	2.299	68.7702	2.640	68.9535
3.078	67.6671	2.255	67.8293	2.285	68.5988	2.301	68.7741	2.731	68.9578
2.967	67.6708	2.253	67.8330	2.313	68.6028	2.299	68.7786	2.831	68.9617
2.864	67.6745	2.257	67.8370	2.308	68.6067	2.294	68.7825	2.938	68.9658
2.765	67.6782	2.253	67.8407	2.313	68.6112	2.297	68.7877	3.042	68.9696
2.667	67.6819	2.262	67.8449	2.330	68.6155	2.299	68.7916	3.156	68.9737
2.588	67.6857	2.261	67.8486	2.345	68.6199	2.302	68.8029	3.200	68.9776
2.516	67.6898	2.264	67.8527	2.351	68.6254	2.303	68.8068	3.190	68.9826
2.452	67.6935	2.264	67.8565	2.361	68.6294	2.300	68.8110	3.151	68.9865
2.406	67.6973	2.270	67.8602	2.370	68.6334	2.305	68.8149	3.059	68.9904
2.359	67.7010	2.269	67.8639	2.378	68.6382	2.300	68.8192	2.975	68.9943
2.325	67.7047	2.276	67.8682	2.384	68.6422	2.304	68.8231	2.840	68.9986
2.308	67.7085	2.273	67.8719	2.388	68.6465	2.299	68.8271	2.741	69.0024
2.309	67.7122	2.277	67.8757	2.383	68.6510	2.302	68.8310	2.635	69.0066
2.308	67.7159	2.277	67.8794	2.383	68.6568	2.307	68.8351	2.562	69.0105
2.295	67.7216	2.283	67.8833	2.374	68.6610	2.302	68.8390	2.489	69.0146
2.298	67.7253	2.281	67.8870	2.375	68.6649	2.306	68.8432	2.415	69.0185
2.288	67.7292	2.292	67.8919	2.365	68.6694	2.309	68.8471	2.363	69.0225
2.292	67.7329	2.290	67.8957	2.359	68.6733	2.305	68.8513	2.325	69.0264
2.286	67.7366								
VDM	**VHJD 2455400 +**	**VDM**	**VHJD 2455400 +**	**VDM**	**VHJD 2455400 +**	**VDM**	**VHJD 2455400 +**	**VDM**	**VHJD 2455400 +**
2.454	67.5912	2.401	67.7342	2.408	67.8970	2.520	68.6662	2.443	68.8526
2.454	67.6005	2.397	67.7380	2.408	67.9007	2.512	68.6707	2.452	68.8565
2.462	67.6033	2.399	67.7417	2.405	67.9045	2.497	68.6746	2.444	68.8607
2.455	67.6063	2.395	67.7455	2.414	67.9084	2.495	68.6789	2.451	68.8646
2.466	67.6091	2.400	67.7492	2.417	67.9121	2.475	68.6828	2.455	68.8688
2.479	67.6118	2.392	67.7533	2.417	67.9164	2.461	68.6871	2.458	68.8727
2.509	67.6143	2.389	67.7571	2.414	67.9201	2.448	68.6910	2.460	68.8767
2.528	67.6169	2.394	67.7617	2.417	67.9244	2.442	68.6951	2.459	68.8806
2.566	67.6194	2.387	67.7654	2.416	67.9281	2.436	68.6990	2.462	68.8876
2.599	67.6220	2.380	67.7693	2.424	67.9319	2.432	68.7031	2.467	68.8915
2.642	67.6245	2.381	67.7730	2.433	67.9357	2.433	68.7070	2.466	68.8959
2.702	67.6281	2.379	67.7768	2.426	67.9395	2.434	68.7128	2.471	68.8998
2.750	67.6307	2.378	67.7805	2.430	67.9432	2.434	68.7167	2.465	68.9039
2.807	67.6332	2.378	67.7843	2.440	67.9473	2.430	68.7217	2.478	68.9078
2.854	67.6360	2.383	67.7880	2.445	67.9510	2.435	68.7256	2.480	68.9126
2.920	67.6386	2.380	67.7918	2.466	67.9548	2.434	68.7310	2.482	68.9165
3.002	67.6411	2.381	67.7955	2.477	67.9586	2.434	68.7349	2.475	68.9208
3.068	67.6440	2.378	67.7992	2.485	67.9624	2.436	68.7389	2.490	68.9247
3.140	67.6469	2.374	67.8029	2.497	67.9661	2.429	68.7428	2.481	68.9287

Table 1
(Continued)

VDM	VHJD 2455400 +	VDM	VHJD 2455400 +	VDM	VHJD 2455400 +	VDM	VHJD 2455400 +	VDM	VHJD 2455400 +
3.206	67.6497	2.374	67.8077	2.513	67.9699	2.432	68.7468	2.483	68.9326
3.257	67.6535	2.376	67.8114	2.527	67.9736	2.436	68.7507	2.535	68.9380
3.252	67.6572	2.375	67.8152	2.531	67.9777	2.435	68.7547	2.573	68.9419
3.233	67.6609	2.381	67.8190	2.534	67.9814	2.430	68.7586	2.716	68.9509
3.202	67.6646	2.377	67.8230	2.535	67.9893	2.430	68.7633	2.794	68.9548
3.107	67.6684	2.381	67.8267	2.540	67.9918	2.436	68.7672	2.872	68.9591
3.017	67.6721	2.374	67.8306	2.432	68.5935	2.430	68.7715	2.961	68.9630
2.918	67.6758	2.380	67.8343	2.436	68.5963	2.428	68.7753	3.079	68.9670
2.824	67.6796	2.379	67.8383	2.441	68.6002	2.427	68.7799	3.183	68.9709
2.754	67.6833	2.378	67.8420	2.435	68.6041	2.432	68.7838	3.241	68.9750
2.677	67.6870	2.380	67.8462	2.440	68.6080	2.432	68.7890	3.265	68.9789
2.604	67.6911	2.381	67.8499	2.456	68.6125	2.431	68.7929	3.263	68.9839
2.548	67.6948	2.392	67.8541	2.480	68.6168	2.432	68.8082	3.205	68.9878
2.505	67.6986	2.380	67.8578	2.485	68.6212	2.439	68.8123	3.127	68.9917
2.460	67.7023	2.388	67.8615	2.510	68.6267	2.439	68.8162	3.013	68.9956
2.437	67.7061	2.386	67.8653	2.517	68.6307	2.442	68.8205	2.939	68.9998
2.433	67.7098	2.393	67.8695	2.525	68.6347	2.442	68.8244	2.823	69.0037
2.424	67.7135	2.394	67.8732	2.536	68.6395	2.440	68.8284	2.737	69.0079
2.415	67.7172	2.396	67.8770	2.540	68.6435	2.443	68.8323	2.668	69.0118
2.409	67.7230	2.390	67.8808	2.537	68.6478	2.440	68.8364	2.592	69.0159
2.415	67.7267	2.402	67.8846	2.537	68.6523	2.444	68.8403	2.536	69.0198
2.411	67.7305	2.406	67.8883	2.530	68.6581	2.439	68.8445	2.491	69.0238
		2.402	67.8933	2.530	68.6623	2.445	68.8484	2.452	69.0277

RDM	RHJD 2455400 +	RDM	RHJD 2455400 +	RDM	RHJD 2455400 +	RDM	RHJD 2455400 +	RDM	RHJD 2455400 +
2.489	67.5927	2.432	67.7349	2.433	67.8939	2.563	68.6668	2.446	68.8532
2.481	67.6011	2.433	67.7386	2.434	67.8976	2.542	68.6714	2.448	68.8571
2.481	67.6039	2.430	67.7423	2.436	67.9014	2.530	68.6752	2.453	68.8614
2.475	67.6069	2.428	67.7461	2.443	67.9051	2.519	68.6796	2.461	68.8652
2.497	67.6097	2.422	67.7499	2.444	67.9090	2.498	68.6834	2.453	68.8695
2.503	67.6123	2.426	67.7540	2.441	67.9128	2.479	68.6877	2.456	68.8734
2.529	67.6148	2.417	67.7577	2.435	67.9170	2.467	68.6916	2.461	68.8773
2.558	67.6173	2.415	67.7623	2.448	67.9207	2.460	68.6958	2.460	68.8812
2.594	67.6199	2.414	67.7660	2.438	67.9251	2.451	68.6996	2.469	68.8882
2.629	67.6224	2.413	67.7699	2.445	67.9288	2.448	68.7038	2.465	68.8921
2.663	67.6250	2.409	67.7736	2.447	67.9326	2.455	68.7076	2.468	68.8965
2.729	67.6286	2.407	67.7775	2.452	67.9363	2.447	68.7134	2.470	68.9004
2.778	67.6311	2.409	67.7812	2.456	67.9401	2.444	68.7173	2.472	68.9045
2.825	67.6337	2.405	67.7849	2.460	67.9438	2.450	68.7224	2.477	68.9084
2.880	67.6365	2.409	67.7887	2.462	67.9479	2.448	68.7263	2.479	68.9132
2.929	67.6390	2.412	67.7924	2.485	67.9517	2.449	68.7317	2.479	68.9171
2.996	67.6416	2.402	67.7961	2.503	67.9555	2.448	68.7355	2.480	68.9215
3.065	67.6446	2.409	67.7999	2.505	67.9592	2.445	68.7396	2.482	68.9254
3.143	67.6474	2.402	67.8036	2.518	67.9630	2.444	68.7435	2.485	68.9294
3.199	67.6503	2.408	67.8083	2.535	67.9668	2.447	68.7475	2.497	68.9332
3.219	67.6541	2.397	67.8120	2.565	67.9705	2.448	68.7514	2.547	68.9387
3.219	67.6578	2.403	67.8159	2.584	67.9742	2.447	68.7554	2.588	68.9426
3.209	67.6616	2.400	67.8196	2.591	67.9783	2.447	68.7593	2.722	68.9516
3.150	67.6653	2.405	67.8236	2.592	67.9821	2.441	68.7640	2.800	68.9555
3.081	67.6690	2.403	67.8274	2.591	67.9898	2.449	68.7679	2.888	68.9598
2.990	67.6727	2.401	67.8312	2.591	67.9924	2.445	68.7721	2.968	68.9637
2.900	67.6765	2.404	67.8349	2.446	68.5969	2.442	68.7760	3.064	68.9677
2.817	67.6802	2.403	67.8390	2.443	68.6008	2.443	68.7806	3.163	68.9716
2.738	67.6839	2.404	67.8427	2.455	68.6048	2.422	68.7845	3.217	68.9757
2.679	67.6876	2.407	67.8468	2.461	68.6087	2.445	68.7896	3.216	68.9796
2.610	67.6918	2.413	67.8505	2.479	68.6131	2.446	68.7935	3.212	68.9845
2.560	67.6955	2.406	67.8547	2.494	68.6174	2.447	68.8088	3.159	68.9884
2.515	67.6992	2.418	67.8584	2.514	68.6218	2.452	68.8129	3.066	68.9924
2.488	67.7029	2.409	67.8622	2.537	68.6274	2.440	68.8168	2.982	68.9963
2.461	67.7067	2.414	67.8659	2.551	68.6313	2.439	68.8212	2.884	69.0005
2.453	67.7104	2.425	67.8702	2.574	68.6354	2.449	68.8251	2.795	69.0044
2.447	67.7142	2.417	67.8739	2.584	68.6402	2.450	68.8290	2.722	69.0086
2.439	67.7179	2.421	67.8777	2.598	68.6441	2.449	68.8329	2.642	69.0125

Table 1
(Continued)

RDM	RHJD 2455400+	RDM	RHJD 2455400+	RDM	RHJD 2455400+	RDM	RHJD 2455400+	RDM	RHJD 2455400+
2.438	67.7236	2.427	67.8814	2.590	68.6485	2.449	68.8371	2.591	69.0166
2.440	67.7273	2.423	67.8852	2.594	68.6530	2.452	68.8410	2.533	69.0205
2.439	67.7311	2.431	67.8890	2.590	68.6587	2.450	68.8452	2.501	69.0245
				2.575	68.6630	2.451	68.8491	2.460	69.0284
IDM	IHJD 2455400+	IDM	IHJD 2455400+	IDM	IHJD 2455400+	IDM	IHJD 2455400+	IDM	IHJD 2455400+
2.502	67.6015	2.470	67.7391	2.469	67.8981	2.604	68.6720	2.480	68.8497
2.505	67.6044	2.466	67.7428	2.473	67.9019	2.581	68.6759	2.492	68.8539
2.504	67.6073	2.472	67.7467	2.468	67.9056	2.556	68.6802	2.485	68.8577
2.527	67.6101	2.465	67.7504	2.477	67.9096	2.542	68.6841	2.488	68.8620
2.534	67.6127	2.454	67.7545	2.485	67.9133	2.518	68.6884	2.491	68.8659
2.559	67.6152	2.457	67.7582	2.480	67.9175	2.509	68.6923	2.483	68.8701
2.583	67.6178	2.445	67.7628	2.482	67.9212	2.493	68.6964	2.493	68.8740
2.623	67.6203	2.454	67.7665	2.482	67.9256	2.495	68.7003	2.493	68.8780
2.657	67.6229	2.452	67.7704	2.495	67.9293	2.492	68.7044	2.491	68.8819
2.685	67.6254	2.449	67.7741	2.492	67.9331	2.485	68.7083	2.496	68.8889
2.741	67.6290	2.449	67.7780	2.484	67.9368	2.494	68.7141	2.496	68.8928
2.797	67.6315	2.447	67.7817	2.490	67.9406	2.485	68.7180	2.502	68.8972
2.840	67.6341	2.444	67.7855	2.500	67.9443	2.486	68.7230	2.506	68.9011
2.878	67.6369	2.447	67.7892	2.519	67.9485	2.492	68.7269	2.501	68.9052
2.935	67.6395	2.452	67.7929	2.528	67.9522	2.487	68.7323	2.504	68.9091
2.994	67.6420	2.452	67.7966	2.559	67.9560	2.484	68.7362	2.504	68.9139
3.065	67.6450	2.455	67.8004	2.573	67.9597	2.474	68.7402	2.501	68.9178
3.108	67.6479	2.448	67.8041	2.603	67.9635	2.488	68.7441	2.513	68.9221
3.164	67.6507	2.440	67.8088	2.626	67.9673	2.471	68.7481	2.510	68.9260
3.174	67.6546	2.447	67.8126	2.641	67.9710	2.484	68.7520	2.516	68.9300
3.167	67.6583	2.443	67.8164	2.659	67.9747	2.476	68.7560	2.522	68.9339
3.158	67.6621	2.438	67.8201	2.672	67.9789	2.478	68.7599	2.571	68.9393
3.115	67.6658	2.448	67.8242	2.687	67.9902	2.471	68.7646	2.611	68.9432
3.056	67.6695	2.454	67.8279	2.673	67.9928	2.482	68.7685	2.742	68.9522
2.960	67.6732	2.447	67.8318	2.487	68.5975	2.477	68.7728	2.805	68.9561
2.880	67.6770	2.447	67.8355	2.488	68.6014	2.471	68.7766	2.886	68.9604
2.816	67.6807	2.446	67.8395	2.504	68.6054	2.470	68.7812	2.970	68.9643
2.745	67.6844	2.444	67.8432	2.511	68.6093	2.477	68.7851	3.048	68.9683
2.690	67.6881	2.441	67.8473	2.517	68.6138	2.467	68.7903	3.123	68.9722
2.637	67.6923	2.445	67.8511	2.548	68.6181	2.465	68.7942	3.168	68.9763
2.585	67.6960	2.446	67.8552	2.572	68.6225	2.482	68.8055	3.171	68.9802
2.531	67.6997	2.452	67.8590	2.609	68.6280	2.474	68.8094	3.159	68.9852
2.511	67.7034	2.444	67.8627	2.632	68.6320	2.481	68.8136	3.100	68.9891
2.487	67.7072	2.453	67.8664	2.648	68.6360	2.471	68.8175	3.031	68.9930
2.490	67.7109	2.452	67.8707	2.668	68.6408	2.479	68.8218	2.964	68.9969
2.472	67.7147	2.467	67.8744	2.664	68.6448	2.482	68.8257	2.878	69.0011
2.472	67.7184	2.462	67.8782	2.679	68.6491	2.478	68.8297	2.789	69.0050
2.487	67.7241	2.456	67.8819	2.662	68.6536	2.478	68.8336	2.721	69.0092
2.471	67.7278	2.456	67.8858	2.665	68.6594	2.480	68.8377	2.658	69.0131
2.467	67.7317	2.461	67.8895	2.645	68.6636	2.484	68.8416	2.584	69.0172
2.468	67.7354	2.469	67.8944	2.629	68.6675	2.476	68.8458	2.545	69.0211
								2.517	69.0251

is strong magnetic activity. It seems to have spots as we might expect for a solar-type short period binary. The difference in eclipse depths ranges from $I = 0.5$ mag to $B = 0.8$ mag. These values are those of an EA binary.

For the Check star, both TYCHO $B - V$ and 2MASS $V - K$, $J - H$, and $H - K$ (Cox 2000) agree on a K1-K5V spectral type. Our instrumental $V - K$ $(B - V)$ measured values also agree with the 2MASS results given in Table 4. Based off of these results and from the confirmation of heavy solar type activity, we used a primary temperature of 5000 K in our light curve models. Despite the formal errors given in the table, we believe that the uncertainty on this temperature is nearer ±500 K.

7. LIGHT CURVE SOLUTIONS

A four color, BVR_cI_c, simultaneous synthetic light curve solution was undertaken. Binary Maker 3.0 (Bradstreet & Steelman 2002) was used to explore the character of our light curves and determine initial parameters of each of the B, V, R_c, I_c light curves. Next, the mean values from the fits generated a set of starting values for the Wilson code (Wilson & Devinney 1971 (WD); Wilson 1990, 1994; Van Hamme & Wilson 1998; Wilson & Van Hamme 1993). This version includes Kurucz atmospheres, rather than black body, and a detailed reflection treatment along with two-dimensional

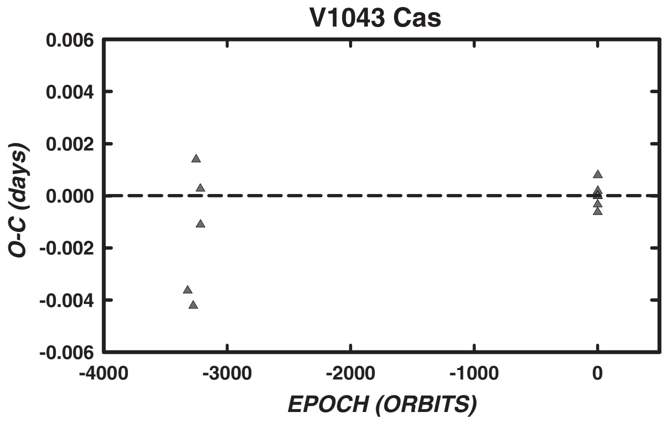

Figure 4. $O - C$ residuals of V1043 Cas from Equation (2).

Table 2
Eclipse Timings and Linear Residuals, V1043 CAS from Equation (2)

No.	Epochs	Cycles	Weight	$O - C$	Reference
1	53252.011	−3349.0	0.1	0.0064	Nakajima et al. 2006
2	53271.187	−3320.0	0.1	−0.0036	Nakajima et al. 2006
3	53300.9578	−3275.0	0.2	−0.0042	Nakajima et al. 2006
4	53316.1799	−3252.0	1.0	0.0014	Nakajima et al. 2006
5	53339.9945	−3216.0	1.0	−0.0011	Nakajima et al. 2006
6	53339.0035	−3217.5	1.0	0.0003	Nakajima et al. 2006
7	55467.6564(09)	0.0	1.0	−0.0003	SAMEC/SMITH
8	55467.9869(39)	0.5	1.0	−0.0006	SAMEC/SMITH
9	55468.6493(28)	1.5	1.0	0.0002	SAMEC/SMITH
10	55468.9807(08)	2.0	1.0	0.0008	SAMEC/SMITH

Table 3
Light Curve Characteristics, V1043 Cas

Filter	Min I		Max I	
	Phase	(mag)	Phase	(mag)
ΔB	00	3.200 ± 0.009	0.25	2.246 ± 0.038
ΔV		3.263 ± 0.011		2.374 ± 0.032
ΔR_c		3.219 ± 0.08		2.397 ± 0.005
ΔI_c		3.174 ± 0.005		2.438 ± 0.005
Filter	Min II		Max II	
	Phase	(mag)	Phase	(mag)
ΔB	0.50	2.409 ± 0.010	0.75	2.299 ± 0.023
ΔV		2.540 ± 0.021		2.431 ± 0.047
ΔR_c		2.598 ± 0.07		2.439 ± 0.006
ΔI_c		2.687 ± 0.008		2.471 ± 0.004
Filter		Min I−Max I		Min I−Min II
ΔB		0.954 ± 0.047		0.791 ± .019
ΔV		0.889 ± 0.043		0.723 ± 0.02
ΔR_c		0.822 ± 0.033		0.621 ± 0.065
ΔI_c		0.736 ± 0.010		0.487 ± 0.013
Filter		Max II−Max I		Min II−Max I
ΔB		0.053 ± 0.61		0.163 ± 0.048
ΔV		0.057 ± 0.079		0.166 ± 0.053
ΔR_c		0.042 ± 0.011		0.201 ± 0.042
ΔI		0.042 ± 0.009		0.249 ± 0.013

limb-darkening coefficients. The differential corrections routine was iterated a number of times until convergence was achieved for a solution. Since the eclipses were not total, we undertook a mass ratio ($q = m_2/m_1$) search to determine the best-fitting range of q-values. An extensive q-search revealed that the best mass ratio fit was near 0.9, as shown in Figure 6.

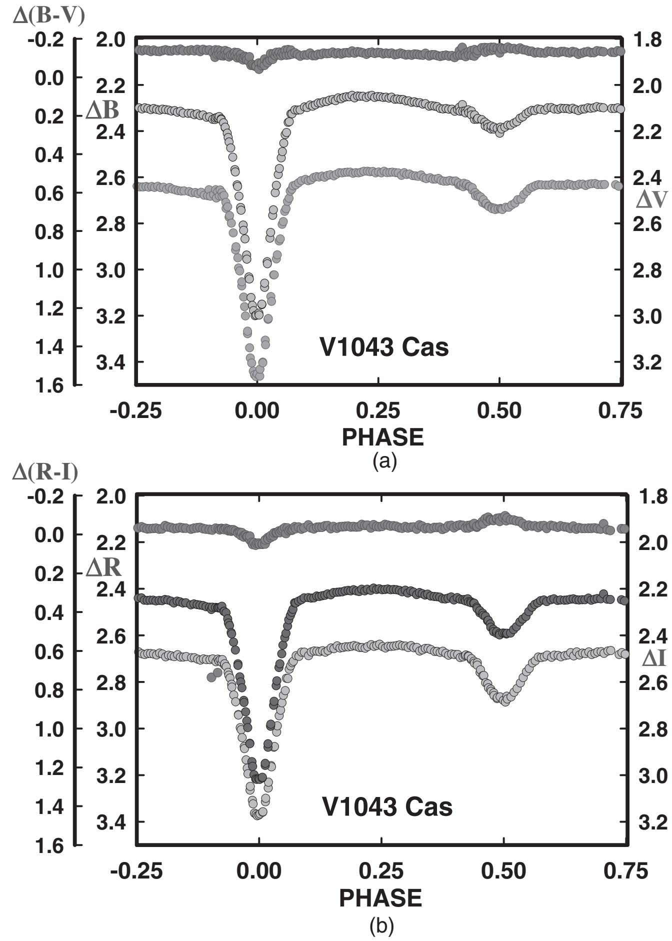

Figure 5. (a) B, V Delta Mags of V1043 Cas Phased with Equation (2). (b) R, I Delta Mags of V1043 Cas Phased with Equation (2).

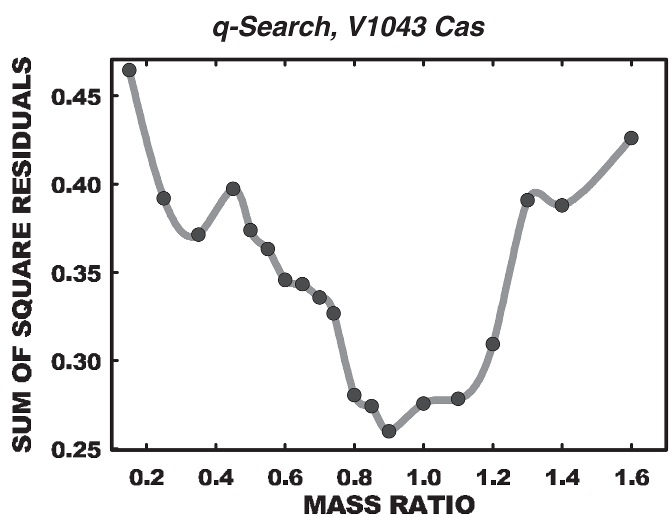

Figure 6. Mass ratio search for V1043 Cas minimizes at about 0.9.

From Binary Maker, we found two spots were needed to fit the asymmetries of the light curve, one on the primary and one on the secondary. Our final spot parameters revealed a large 32° radius underluminous cool region with a T-factor of 0.93 on the primary component and a large superluminous region, a plage, with a T-factor of 1.165 on the secondary component. We have

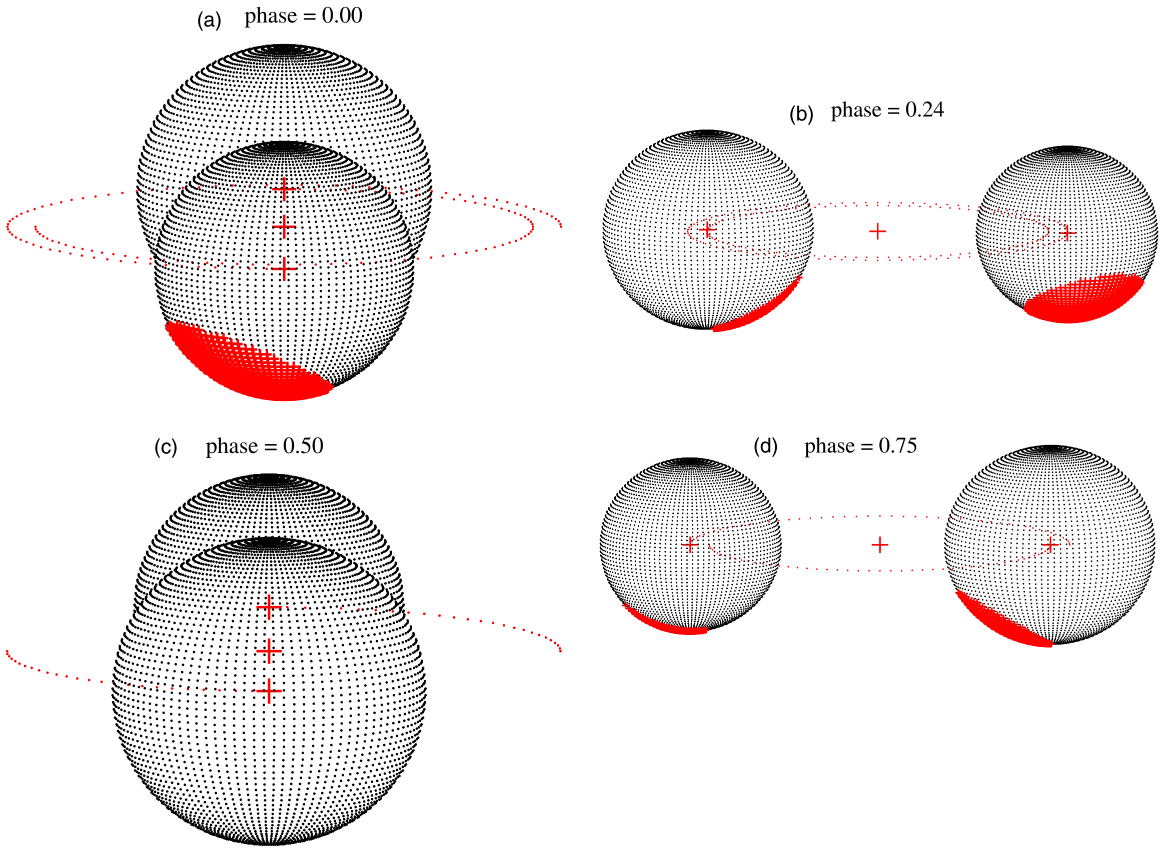

Figure 7. (a) Geometrical representation of V1043 Cas at phase 0.00. (b) Geometrical representation of V1043 Cas at phase 0.24. (c) Geometrical representation of V1043 Cas at phase 0.50. (d) Geometrical representation of V1043 Cas at phase 0.75.

(A color version of this figure is available in the online journal.)

Table 4
2MASS Photometry for V1043 Cas

Filter	Mag	Color Index	Value	Spectral Type	Temperature
J	11.554 ± 0.01	$(J-H)$	0.497 ± 0.041	K2 ± 2	5000 ± 200 K
H	11.057 ± 0.02	$(H-K)$	0.097 ± 0.035	K3 ± 4	4850 ± 600 K
K	10.960 ± 0.021				

Table 5
Synthetic Curve, $q = 0.90$, Solution for V1043 Cas

Parameters	Values	Parameters	Values
ΔB, ΔV, ΔR_c, ΔI_c (nm)	440, 550, 640,790	r_1, r_2 (pole)	0.244 ± 0.002, 0.241 ± 0.064
$x\mathrm{bol}_{1,2}$, $y\mathrm{bol}_{1,2}$	0.643, 0.475, 0.160, 0.284	r_1, r_2 (point)	0.255 ± 0.002, 0.252 ± 0.001
$x_{1I,2I}$, $y_{1I,2I}$	0.591, 0.697, 0.183, 0.325	r_1, r_2 (side)	0.248 ± 0.002, 0.244 ± 0.001
$x_{1R,2R}$, $y_{1R,2R}$	0.686, 0.784, 0.165, 0.290	r_1, r_2 (back)	0.253 ± 0.002, 0.250 ± 0.001
$x_{1V,2V}$, $y_{1V,2V}$	0.778, 0.837, 0.108, 0.32	SPOT 1	STAR 1 (Cool Spot)
$x_{1B,2B}$, $y_{1B,2B}$	0.847, 0.869, -0.018, 0.321	colatitude	147°.0 ± 0°.6
g_1, g_2	0.32, 0.32	Longitude	12°.1 ± 0°.7
A_1, A_2	0.50, 0.50	Spot radius	32.2 ± 0°.4
Inclination (°)	81.27 ± 0.02	T-Factor	0.933 ± 0.002
T_1, T_2 (K)	5000, 3832 ± 1	SPOT 1	STAR 2 (Hot spot)
Ω_1, Ω_2	4.496 ± 0.003, 4.758 ± 0.003	colatitude	153°.4 ± 0°.3
q (m_2/m_1)	0.899 ± 0.001	Longitude	125°.4 ± 0°.8
Fill-outs: F_1, F_2	80%, 75%	Spot radius	42°.2 ± 0°.2
$L_1/(L_1+L_2)_I$	0.7914 ± 0.0006	T-Factor	1.165 ± 0.002
$L_1/(L_1+L_2)_R$	0.8365 ± 0.0004		
$L_1/(L_1+L_2)_V$	0.8716 ± 0.0006	JD0 (days)	2455467.65748 ± 0.00001
$L_1/(L_1+L_2)_B$	0.9100 ± 0.0007	Period (days)	0. 6615992 ± 0. 0000054

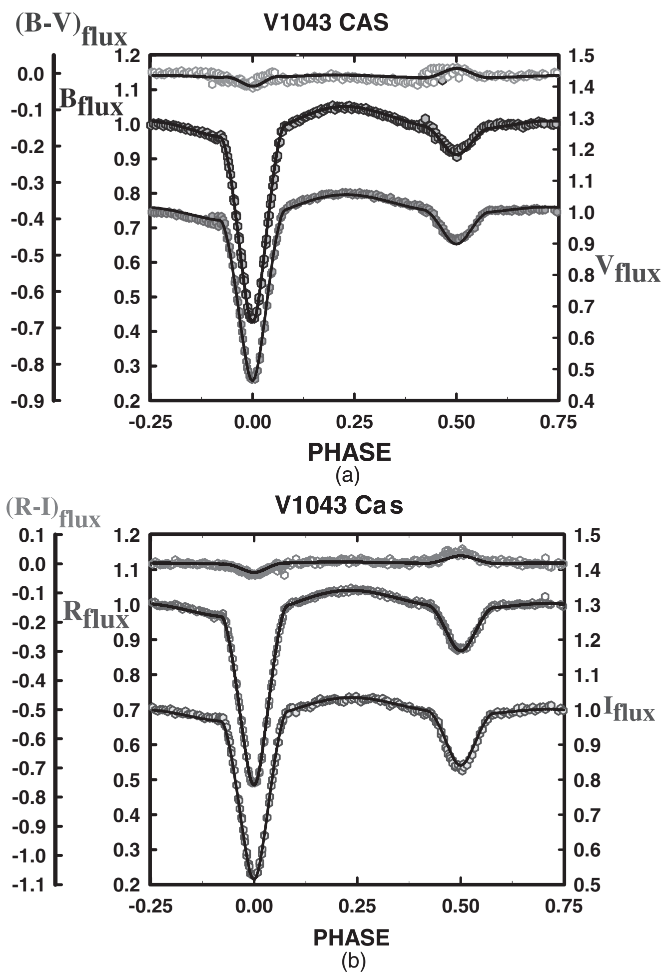

Figure 8. (a) *B* and *V* normalized fluxes overlaid by our solution of V1043 Cas. (b) *R* and *I* normalized fluxes overlaid by our solution of V1043 Cas.

found that hot spots and cool spots occur with about the same frequency on spotted solar-type stars. The solution parameters are given in Table 5. The errors are formal errors generated from the Wilson code for the purpose of convergence. When the absolute values of all of the corrections are less than their associated uncertainties, convergence is achieved, which is the solution. A geometrical representation of the system is given in Figures 7(a)–(d) at quadratures so that the reader may see the placement of the spots and the relative size of the stars as compared to the orbit. As can be seen, the system is well detached. The normalized curves overlaid by our light curve solutions are shown as Figures 8(a) and (b).

8. CONCLUSION

V1043 Cas is interpreted here as an early K-type dwarf binary. It has, surprisingly, an Algol-type light curve belonging to a detached binary system rather than an EW contact binary. Indeed, it could be classified as a PCWB. We recently modeled a shallow contact EB binary (only 8% past critical contact) with G and M components, HO Psc, which was evidently a result of the recent contact of components similar to our present system (Samec et al. 2012b). The mass ratio of our present binary is 0.9 and its fill-outs are 80% and 75%, by potential, of its critical contact Roche lobes for the primary and secondary components, respectively. So, V1043 Cas could also be classified as a near contact binary.

Table 6
Some Precontact (EA) W UMa Binaries

System	*T*1	*T*2	*q*	*P* (days)	Ref.
V1001 Cas	4500	3689	0.38	0.43	Samec et al. 2012a
GU Boo	3800	3700	1.00	0.49	Windmiller & Orosz 2010
V1043 Cas	5000	3832	0.90	0.66	Present Paper
SV Cam	5800	4140	0.64	0.59	Rucinski et al. 2002
UV Leo	6000	5930	0.93	0.60	Popper 1965
ER Vul	5900	5750	0.96	0.70	Hill, et al. 1990
HP Aur	5900	5390	0.80	0.71	Giuricin et al. 1983
AE Cas	5530	4780	0.87	0.76	Srivastava & Kandpal 1984
BH Vir	6250	5625	0.86	0.82	Abt, 1965
WY Cnc	5600	3500	0.38	0.83	Yongpo et al. 2009
FL Lyr	6000	5230	0.79	2.18	Popper et al. 1986
VZ Hya	6410	6120	0.91	2.90	Popper 1965
TY Pyx	5400	5340	0.98	3.20	Andersen & Popper 1974
UZ Dra	6100	5844	0.92	3.27	Lacy et al. 1989
UX Men	6195	6152	0.97	4.18	Anderson et al. 1989
WZ Oph	6200	6220	0.99	4.18	Popper 1965
HD 27130	5470	3977	0.72	5.61	Schiller and Milone 1987
EW Ori	5940	5560	0.97	6.937	Popper et al. 1986
HS Aur	5346	5200	0.98	9.88	Popper et al. 1986
Average	5650	5050	0.826	2.575	

9. A COMMENT ON PCWBs

Using Binary Stars, A Pictorial Atlas (Terrell et al. 1992) as a starting point (see Table 6 for full listing of sources), we have identified about 20 PCWBs. We included only those with spectral types redder than ∼F8V. Thus, they are all solar-type binaries, that is, stars that would be identified as those undergoing magnetic braking. They are sorted by orbital period. We note that the periods range from an ∼10 to ∼0.4 day period for V1001 Cas (Samec et al. 2012a). Somewhere below this period, the components become semidetached, then shallow contact and over contact systems and finally fast rotating single stars. The average mass ratio is about 0.8. This is interesting, since mass ratios seem to decrease to under 0.1 in extreme mass ratio binaries, which are thought to be near final coalescence. Perhaps close binary stars start out with similar masses and become more extreme as time goes on, as would be expected if binary coalescence is actually a reality and one star is subsumed by its more massive companion. ΔT's (the difference in temperatures of the components) have different a story. These average about 100 K and become more disparate until the final stages when they average about 250 K due to the high fill-out common atmosphere. We note that SV Cam (Rucinski et al. 2002) is designated as an EA/RS and we find that it has masses of 1.14 and 0.73, which definitely makes it of solar type. ER Vul (Hill et al. 1990), likewise, is made up of 1.1 solar mass components, yet it is a detached RS CVn type binary. Likewise, TY Pyx is listed as an RS CVn type. TY Pyx is thought to be in a pre-main-sequence part of its evolution (Rao & Sarma 1981), which fits the scenario that we suggest. Schiller & Milone (1987) report that HD 27130 has light curve properties of an RS CVn type. This tells us what we may have guessed about W UMa systems, i.e., that they are evolved binaries from highly active counterparts. Thus, it is possible that the same characteristics can be found in semidetached and shallow contact W UMa's.

If we follow their light curves, then we might find that many behave similarly to their counterparts, RS CVn systems. Are W UMa binaries simply evolved RS CVn dwarfs? The small number of identified systems in Table 6 (as compared to the large number of W UMa contact systems) may indicate that perhaps their state of evolution (AML) is so rapid that they are actually rare and that the process slows in the overcontact state. Further investigation and identification of candidate systems is needed.

The publication of this paper is supported by a grant from the R. M. Santilli Foundation. We also thank both NURO and SARA for their allocation of observing time, as well as NASA, the American Astronomical Society, and the Arizona Space grant for their partial support of travel expenses. We also thank USC, Lancaster for their support of our association with NURO.

REFERENCES

Abt, H. 1965, PASP, 77, 367

Andersen, J., & Popper, D. M. 1974, A&A, 39, 131

Anderson, J., Clausen, J. V., & Magain, P. 1989, A&A, 211, 346

Bradstreet, D. H., & Steelman, D. P. 2002, BAAS, 34, 1224

Cox, A. N. (ed.) 2000, Allen's Astrophysical Quantities (4th ed.; New York: Springer)

Giuricin, G., Mardirossian, F. D., & Mezzetti, M. 1983, AcA, 33, 159

Guinan, E. F., & Bradstreet, D. H. 1988, in Proc. NATO Advanced Study Institute, held at Viana do Castelo, Portugal, 1987 September 21–October 2, Kinematic Clues to the Origin and Evolution of Low Mass Contact Binaries, Formation and Evolution of Low Mass Stars, ed. A. K. Dupree & M. T. V. T. Lago (NATO Advanced Science Institutes (ASI) Series C, Vol. 241; Dordrecht: Kluwer), 345

Hill, G., Fisher, W. A., & Holmgren, D. 1990, A&A, 238, 145

Kazarovets, E. V., Samus, N. N., Durlevich, O. V., Kireeva, N. N., & Pastukhova, E. N. 2011, IBVS, 5969, 1

Lacy, C. H., Gülmen, O., Necdet, G., & Sezer, C. 1989, AJ, 97, 822

Nakajima, K., Yoshida, S., & Ohkura, N. 2006, IBVS, 5700, 16

Popper, D. M. 1965, ApJ, 141, 126

Popper, D. M., Lacy, C. H., Frueh, M. L., & Turner, A. E. 1986, AJ, 91, 383

Rao, P. V., & Sarma, M. B. K. 1981, AcA, 31, 107

Rucinski, S. M., Lu, W., Capobianco, C., Mochnaki, S.W., et al. 2002, AJ, 124, 1738

Samec, R. G., Chamberlain, H. A., Figg, E. R., et al. 2012a, in The Observatory, Vol. 132, A Photometric Study of the Dwarf Algol Binary, V1001 Cassiopeia

Samec, R. G., Smith, P. M., Robb, R., Faulkner, D. R., & Van Hamme, W. 2012b, PASP, 124, 693

Schiller, S. J., & Milone, E. F. 1987, AJ, 93, 1471

Srivastava, J. R., & Kandpal, C. D. 1984, AcA, 34, 281

Terrell, D., Mukherjee, J., & Wilson, R. E. 1992, Binary Stars, A Pictorial Atlas (Malabar, FL: Krieger)

Wilson, R. E. 1990, ApJ, 356, 613

Wilson, R. E. 1994, PASP, 106, 921

Wilson, R. E., & Devinney, E. J. 1971, ApJ, 166, 605

Wilson, R. E., & Van Hamme, W. 1993, AJ, 106, 2096

Windmiller, G., & Orosz, J. A. 2010, ApJ, 712, 1003

Van Hamme, W. V., & Wilson, R. E. 1998, BAAS, 30, 1402

Yongpo, T., Xang, F., Xie, W., & Tao, X. 2009, PASJ, 61, 675